Nonlinear Dyn
https://doi.org/10.1007/s11071-018-4486-5

ORIGINAL PAPER

A new nonlinear vibration model of fiber-reinforced composite thin plate with amplitude-dependent property

Hui li · Pengcheng Xue · Zhongwei Guan · Qingkai Han · Bangchun Wen

Received: 11 January 2018 / Accepted: 19 July 2018

Abstract In this paper, the material nonlinearity is introduced in the dynamic modeling of fiber-reinforced composite thin plates, and a new nonlinear vibration model of such composite plate structures with amplitude-dependent property is established with the consideration of the nonlinear stiffness and damping characteristics, which is observed and confirmed in the nonlinear vibration characterization experiment. In this new model, the elastic moduli and loss factors are expressed as the function of strain energy density on the basis of Jones–Nelson material nonlinear model. By using the identified parameters under different excitation amplitudes, these elastic moduli and loss factors are characterized as the function of the maximum dimensionless strain energy density. Then, the power function fitting technique is used to determine the nonlinear stiffness and damping parameters in the model, and the nonlinear natural frequencies, vibration responses and damping ratios of a TC300 carbon/epoxy composite thin plate are calculated and measured in a case study. The comparisons between the theoretical and experimental results show that the maximum calculation error of natural frequencies with consideration of amplitude-dependent property is less than 4.3%, and the maximum calculation errors of resonant response and damping results are no more than 12.5 and 9.6% in the 3rd mode and the 6th mode, respectively. Therefore, the practicability and reliability of the proposed model have been verified.

Keywords Nonlinear vibration model · Fiber-reinforced composite thin plate · Nonlinear vibration · Amplitude-dependent property · Strain energy density

H. Li (✉) · P. Xue · Q. Han · B. Wen
School of Mechanical Engineering and Automation, Northeastern University, Shenyang 110819, China
e-mail: lh200300206@163.com

P. Xue
e-mail: 1690452186@qq.com

Q. Han
e-mail: han29@foxmail.com

B. Wen
e-mail: bcwen1930@vip.sina.com

H. Li · Z. Guan
School of Engineering, University of Liverpool, Brownlow Street, Liverpool L69 3GQ, United Kingdom
e-mail: lh200300206@163.com

Z. Guan
e-mail: Zhongwei.Guan@liverpool.ac.uk

1 Introduction

The fiber-reinforced composite has excellent mechanical properties, good thermal stability and capability on weight reduction, which is widely used in the aeronautics, astronautics, naval vessels and weapon industries [1]. Currently, there are a large number of such composite thin plate structures, including the solar panels, aircraft engine fan blades, large wind turbine blades, etc. As these plate-like composite structures often work on the harsh environments, their vibration problems

Journal: 11071 MS: 4486 TYPESET DISK LE CP Disp.:2018/7/31 Pages: 23 Layout: Medium

become increasingly severe, such as an excessive vibration, wear and fatigue failure. In addition, with the in-depth research, the fiber-reinforced composite structures are found to show the nonlinear stiffness and damping properties [2–4]. For example, the natural frequencies change with different external excitation levels or strain levels, which show some nonlinear stiffness characteristics, and the damping properties are also closely related to excitation frequencies and excitation levels. These nonlinear characteristics have brought a great deal of difficulties and challenges to the traditional vibration modeling methods, which are mainly dependent on the linear equivalence principle. Therefore, it is of great scientific significance to study the nonlinear vibration characteristics and the corresponding modeling techniques [5].

Nowadays, the nonlinear vibration studies of fiber-reinforced composite thin plate have attracted extensive attentions and most methods are achieved by Von Kármán nonlinear theory. Rao and Pillai [6] analyzed the large-amplitude vibrations of a simply supported composite plate with immovable edges. The Kirchhoff's hypothesis and von Kármán theory were used in the formulation with the in-plane deformation and inertias were considered. It was found that the behavior of the oscillations was the same for both positive and negative displacements and the related frequency ratio would increase with the magnitude of the amplitude. Singh et al. [7] presented a direct numerical integration method of the frequency/time period expression to study the nonlinear vibration behavior of the fiber-reinforced plates also based on the Von Kármán relationship. It was found that the frequency ratio decreased with an increase in modulus ratio, and also was dependent on the amplitude direction. Ribeiro and Petyt [8] studied geometrically nonlinear vibration of thin laminated composite plates under the fully clamped boundary condition by the hierarchical finite element. The Von Kármán nonlinear theory and harmonic balance method were used to solve the nonlinear equations of motion. Chen et al. [9] presented the semi-analytical finite strip method to analyze the geometrically nonlinear response of a rectangular composite laminated plate under the simply supported boundary condition with the von Karman assumptions. The nonlinear dynamic problem was solved by using the Newmark time stepping scheme in association with Newton–Raphson iteration. Lee and Ng [10] proposed a time-domain modal formulation using the finite element method for large-amplitude vibrations of composite thin plates. Also, on the basis of von Kármán theory, the nonlinear free and forced vibration responses were obtained by modal reduction method. Harras et al. [11] established a theoretical model of nonlinear vibration of the thin composite plates based on the von Kármán strain–displacement relationship. The effect of nonlinearity on the nonlinear resonance frequencies and modal shapes associated with bending stress patterns was investigated. Onkar and Yadav [12] conducted the nonlinear random vibration analysis on the composite laminated plate with uncertain material properties. The dynamic equations were obtained based on the Kirchhoff–Love plate theory and Von Kármán strain–displacement relationship. Singha and Daripa [13] studied the large-amplitude vibration behavior of a composite thin plate by finite element method. The nonlinear matrix amplitude equations were obtained by employing Galerkin's method based on the von Kármán's assumption. Zafer and Zahit [14] studied the nonlinear dynamic response of a laminated composite plate under the simply supported boundary condition. The geometric nonlinearity effects were also taken into account with the von Kármán theory. Singha and Daripa [15] used the shear deformable finite element method to analyze the large-amplitude vibration characteristics of composite plates. The nonlinear matrix amplitude equations were also obtained based on the Von Kármán nonlinear strain–displacement relationship.

In addition, several studies are reported on the nonlinear material model of fiber-reinforced composite with other hypotheses in the stress–strain relationship. Hahn and Tsai [16] proposed a mathematical model to describe the inherent nonlinearity in the longitudinal shear in unidirectional composite laminae. An additional fourth-order term of the axial-shear stress was added to the polynomial function to derive the nonlinear stress–strain relationship of fiber composite. Jones, Nelson and Morgan[17,18] proposed a new material model for the deformation behavior of fiber-reinforced composite under static loading. They pointed out that the nonlinear stress–strain behavior was mainly due to the nonlinear matrix material which greatly affected the transverse modulus and the shear modulus. Therefore, the material parameters were expressed as the function of strain energy density. Amijima and Adachi [19] presented a simplified mode to predict the nonlinear stress–strain responses of the unidirectional lamina. By applying the classical laminated plate theory

Journal: 11071 MS: 4486 TYPESET DISK LE CP Disp.:2018/7/31 Pages: 23 Layout: Medium

to the small stress or strain increments of the stress–strain curve, the nonlinear stress–strain curve was continuously predicted for various composite specimens. Mathison et al. [20] established a nonlinear material model using the orthotropic endochronic theory. The model was formulated in terms of elastic constants and endochronic parameters, and all constants and parameters were determined from normal and shear tests on unidirectional and off-axis composite specimens. Tabiei et al. [21] proposed a nonlinear strain rate-dependent composite material model, which can be used for simulating the behavior of composite structures under impact and tensile loadings.

As this paper focuses on amplitude-dependent property of composite materials and structures, some important and selective literatures on this topic were highlighted here. Firle [22] investigated the amplitude dependence of internal friction and shear modulus of boron fibers and found the strong amplitude dependence for higher oscillatory stresses. Maslov and Kinra [23] explored the amplitude–frequency dependence of damping property of carbon foam. The elastic moduli and loss factors were inverted from resonance frequencies and logarithmic decay measurements performed at several normal-mode resonances. Höfer and Lion [24] investigated the dynamic material behavior of filler-reinforced rubber and proposed a frequency- and amplitude-dependent model which can evaluate the stationary stress response in terms of the storage and the loss moduli. Khan et al. [25] studied the damping characteristics of carbon fiber-reinforced composites containing multi-walled carbon nanotubes (CNT). They found that the damping ratio was dependent on the amplitude as a result of the random orientation of CNTs in the epoxy matrix.

Although the above researches have deeply investigated the nonlinear vibration characteristics of fiber-reinforced composite plates, most of them focus on the geometric nonlinearity of composite plates based on the Von Kármán strain–displacement relationship. Besides, a few scholars[17,18] propose a model to clarify the nonlinear stress–strain relationship of fiber-reinforced composite structure. However, their primary concern is the nonlinearity in the field of static loadings. The material nonlinearity has not been introduced in the dynamic modeling of composite structures. Therefore, it is necessary to introduce the material nonlinearity in the nonlinear vibration analysis of such a composite plate, especially to establish an appropriate mathematical model to describe the nonlinear vibration phenomenon with amplitude dependence.

2 Nonlinear vibration characterization experiment

In order to deeply understand nonlinear vibration behavior of fiber-reinforced composite thin plate, in this section, nonlinear vibration characterization experiment is carried out to observe and confirm the nonlinear stiffness and damping phenomenon under different amplitudes. Three different TC300 carbon/epoxy composite plates with the same sizes, namely composite plate A, B and C, are used as test objects, as shown in Fig. 1, which are laminated and produced by Jiangxi Jiujiang Diwei composite materials Co. Ltd. Besides, composite plate A is symmetrically laid with

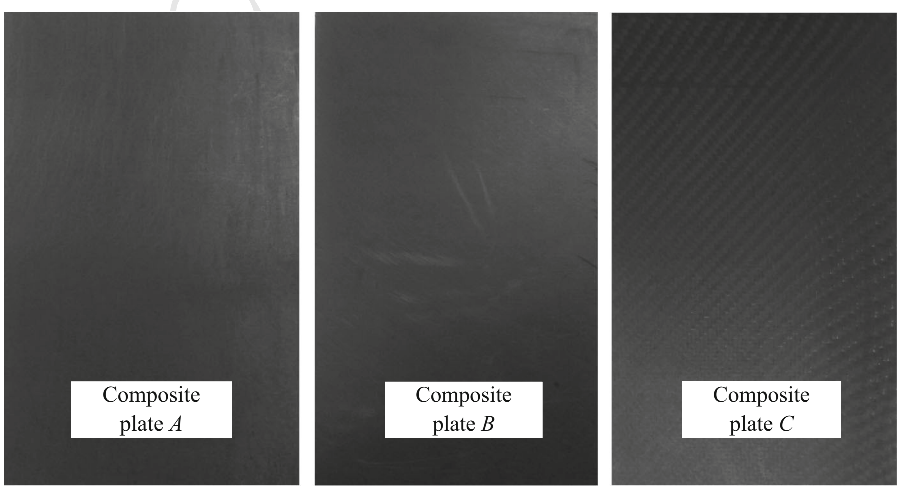

Fig. 1 Three different TC300 carbon/epoxy composite plates

Journal: 11071 MS: 4486 TYPESET DISK LE CP Disp.:2018/7/31 Pages: 23 Layout: Medium

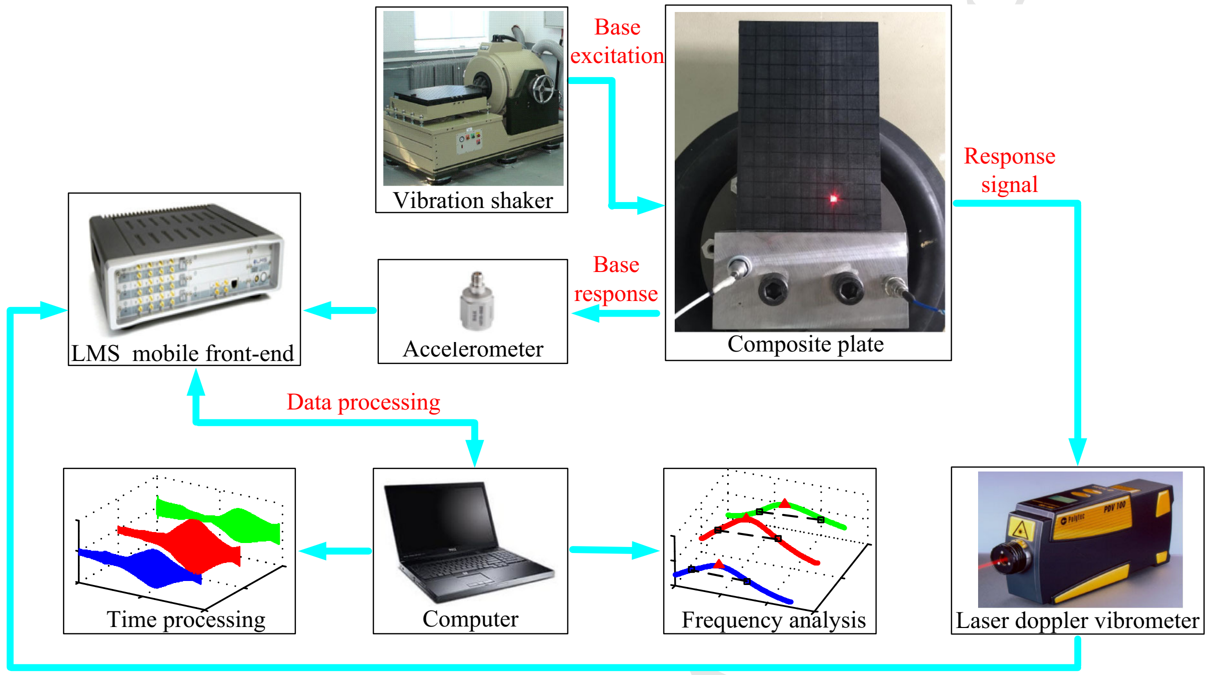

Fig. 2 Schematic of vibration test system of fiber-reinforced composite thin plate

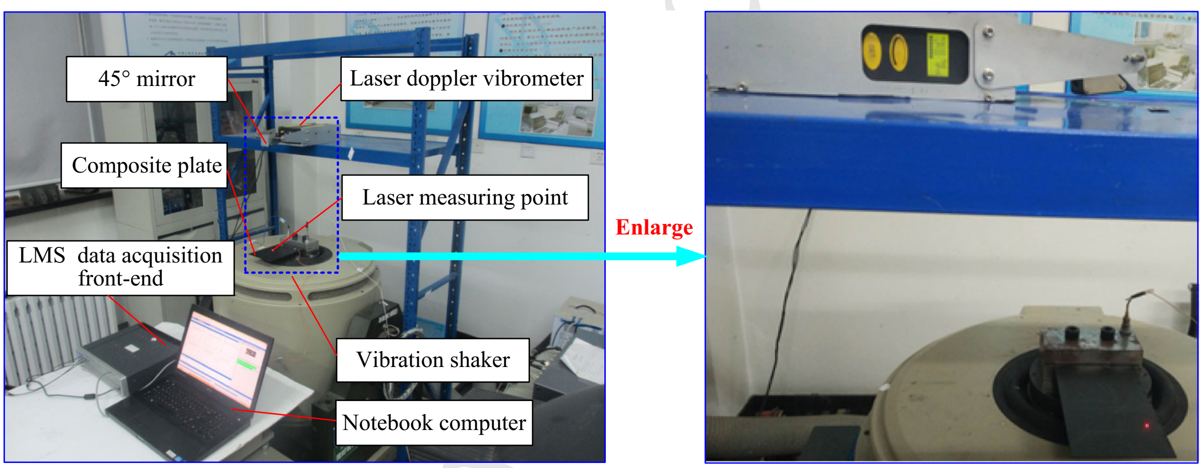

Fig. 3 Real test picture of vibration test system of fiber-reinforced composite thin plate

laminate configuration of $[0/0]_{5\mathrm{s}}$, composite plate B is symmetrically laid with laminate configuration of $[+45/-45]_{5\mathrm{s}}$, and composite plate C is woven fabric composite plate with laying angle of $\pm 45°$.

In order to measure the vibration parameters of the composite plates with high accuracy, a vibration test system is set up in the nonlinear vibration characterization experiment, whose schematic and real test picture can be seen in Figs. 2 and 3. The fixture and M8 bolts are used to clamp the one side of the composite plates so as to simulate cantilever constraint boundary, and the final length, width and thickness of composite plate A, B and C after the clamping is about 230, 130 and 2.36 mm, respectively. King-design EM-1000F vibration shake is used to provide base excitation to the plate specimens with controllable excitation amplitude and frequency. Polytec PDV-100 laser Doppler vibrometer mounted to a rigid support is used to measure response signal

Journal: 11071 MS: 4486 TYPESET DISK LE CP Disp.:2018/7/31 Pages: 23 Layout: Medium

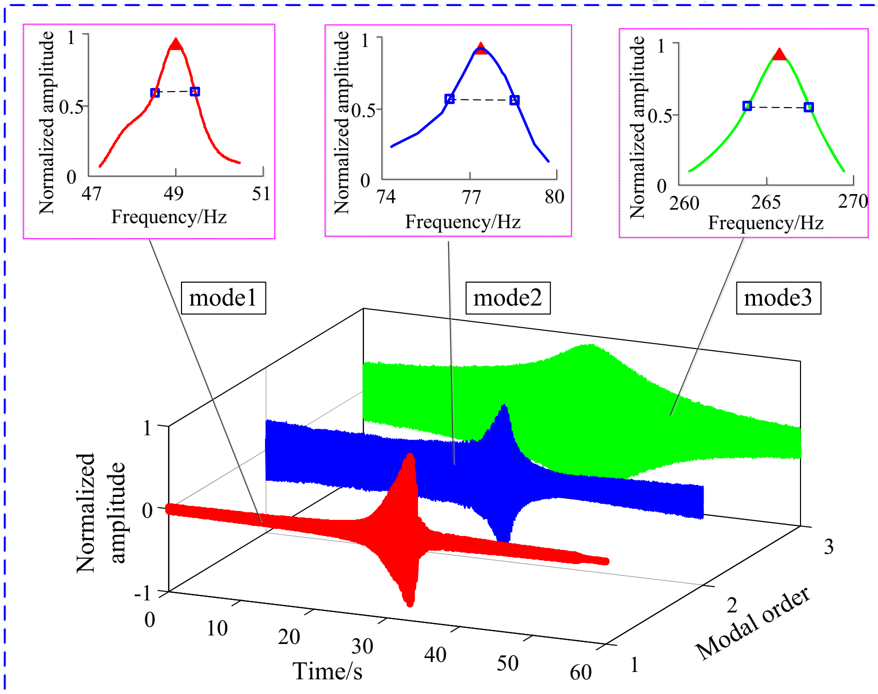

Fig. 4 The first 3 time waveforms and frequency spectrums of composite plate *A* under excitation amplitude of 0.5 g

of the composite plates. The laser measuring point is 170 mm above the constraint end, and the horizontal distance between this point and the left free edge of the plate is 20 mm. In addition, LMS SCADAS 16-channel data acquisition front-end and notebook computer are responsible for recording the laser signal and excitation signal (measured by BK 4514-001 accelerometer).

In the nonlinear vibration characterization experiment, the following measurement steps are adopted. Firstly, the sine sweep test is conducted on the plate specimens with the sweep frequency range of 0–1024 Hz, frequency resolution of 0.125 Hz, and quick sweep speed of 5 Hz/s. Next, after getting the raw response signal, employ the small-segment FFT processing technique [31] to get frequency spectrum of the signal. The first 6 natural frequencies of the plate specimen are roughly determined by identifying the response peak in the spectrum. Then, reselect sweep frequency range which contains each imprecise value of natural frequency and set much slower sweep speed (0.5 Hz/s) to obtain the related frequency spectrum. In this way, by using the half-power bandwidth method, the natural frequencies and damping ratios under the certain excitation amplitude can be identified in the frequency spectrum. Finally, repeat the above measurement steps under different excitation amplitudes (such as 0.1, 0.25, 0.5, 1, 1.5, 2 g), and the nonlinear natural frequencies and modal damping ratios can be measured.

By taking the 1st and 3rd nonlinear characterization test on the composite plate *A* as an example, Fig. 4 shows the first 3 time waveforms and frequency spectrums with the normalized amplitude under excitation amplitude of 0.5 g, and Fig. 5 gives the measured first 3 frequency response spectrums of composite plate *A* under different excitation amplitudes. Then, by applying the half-power bandwidth technique, the first 3 natural frequencies, resonant response and damping ratio results of composite plate *A* are identified under these excitation amplitudes, as shown in Tables 1, 2 and 3. For the convenience of comparison, the corresponding test results of composite plate *B* and *C* are also listed in the same tables.

It can be seen from Fig. 5 and Tables 1, 2 and 3 that the first 3 natural frequencies of three different fiber-reinforced composite thin plates decrease with the increase in base excitation amplitudes in varying degrees, which shows soft nonlinear stiffness charac-

Journal: **11071** MS: **4486** TYPESET DISK LE CP Disp.:**2018/7/31** Pages: **23** Layout: **Medium**

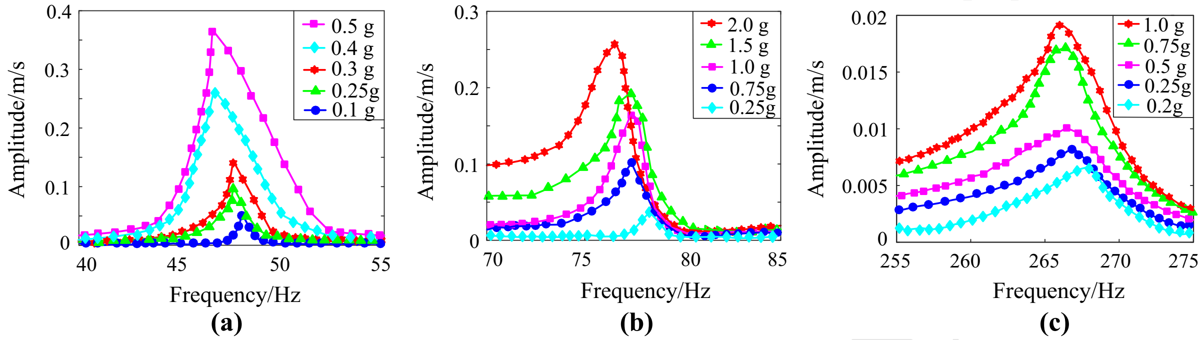

Fig. 5 The first 3 frequency response spectrums of composite plate A under different excitation amplitudes. **a** The 1st frequency response. **b** The 2nd frequency response. **c** The 3rd frequency response

teristics. Besides, it also can be found that the damping results show a rising trend when the excitation amplitudes increase, which shows nonlinear damping variation. Therefore, it can be concluded that the amplitude-dependent property does exist in the vibration behavior of fiber-reinforced composite plates, and it is necessary to establish a theoretical model to explain these nonlinear phenomena.

3 A new nonlinear vibration model with amplitude dependence

In this section, based on Jones–Nelson nonlinear theory, a new theoretical model of fiber-reinforced composite thin plate with amplitude dependence is established by considering both nonlinear stiffness and damping. Also, the theoretical principle and nonlinear vibration solutions are explained in details.

3.1 Theoretical model

Assume that a fiber-reinforced composite thin plate is made of fiber and matrix materials with the total layers of n and density of ρ, as seen in Fig. 6. Firstly, set up the coordinate system xoy at the middle surface, and suppose the length, width and thickness of composite plate are expressed as a , b and h, and the fiber direction within a layer is defined as θ from the x-axis of the coordinate system. In this theoretical model, each layer of the composite plate is located at h_{k-1} and h_k along the z-axis with the equal thickness, "1" represents the direction parallel to the fiber, "2" represents the direction perpendicular to the fiber and "3" represents the direction perpendicular to the 1–2 surface. Meanwhile, assume that the composite plate is under the cantilever boundary condition and is subjected to the base excitation load $y(t)$. w_0 is the vibration displacement in any point $R(x_1, y_1)$, as shown in Fig. 6.

According to the Jones–Nelson nonlinear theory, each elastic modulus of fiber composite can be regarded as the real number, which is actually the function of strain energy density. Then, by using the complex modulus method [26] to introduce the loss factors into this new theoretical model, named as "Jones–Nelson–Hui nonlinear model," the nonlinear material parameters of composite thin plate can be expressed as

$$\begin{aligned} E^*_{\mathrm{non1}} &= E_{\mathrm{non1}} + \mathrm{i}E_1\eta_{\mathrm{non1}} \\ &= E_1\left[\left(1 + A_1 U_{\mathrm{e}}^{\Delta B_1}\right) + i\eta_1\left(1 + C_1 U_{\mathrm{e}}^{\Delta D_1}\right)\right] \end{aligned} \quad (1)$$

$$\begin{aligned} E^*_{\mathrm{non2}} &= E_{\mathrm{non2}} + \mathrm{i}E_2\eta_{\mathrm{non2}} \\ &= E_2\left[\left(1 + A_2 U_{\mathrm{e}}^{\Delta B_2}\right) + \mathrm{i}\eta_2\left(1 + C_2 U_{\mathrm{e}}^{\Delta D_2}\right)\right] \end{aligned} \quad (2)$$

$$\begin{aligned} G^*_{\mathrm{non12}} &= G_{\mathrm{non12}} + \mathrm{i}G_{12}\eta_{\mathrm{non12}} \\ &= G_{12}\left[\left(1 + A_{12} U_{\mathrm{e}}^{\Delta B_{12}}\right) + \mathrm{i}\eta_{12}\left(1 + C_{12} U_{\mathrm{e}}^{\Delta D_{12}}\right)\right] \end{aligned} \quad (3)$$

where E^*_{non1} and E^*_{non2} are the complex elastic moduli of the layer parallel and perpendicular to the fiber, while G^*_{non12} represents the shear modulus in the 1-2 surface. Also, E_{non1}, E_{non2} and G_{non12} are the corresponding real parts of E^*_{non1} , E^*_{non2} and G^*_{non12} , η_{non1} and η_{non2} represent the nonlinear loss factors paralleled and perpendicular to the fiber, and η_{non12} represents the nonlinear loss factor in the 1-2 surface. Moreover, E_1, E_2 and G_{12} are the traditional elastic moduli, η_1, η_2 and η_{12} are traditional loss factors without considering amplitude dependence, U_{e}^{Δ} is the maximum dimensionless strain energy density, A_i and B_i are the nonlinear stiffness

Table 1 The 1st natural frequencies, resonant responses and damping ratios of three composite plates under different excitation amplitudes

Excitation amplitude (g)	Composite plate *A*			Composite plate *B*			Composite plate *C*		
	Natural frequency (Hz)	Resonant response (m/s)	Damping ratio (%)	Natural frequency (Hz)	Resonant response (m/s)	Damping ratio (%)	Natural frequency (Hz)	Resonant response (m/s)	Damping ratio (%)
0.1	48.0	0.0575	1.010	27.7	0.2591	0.989	39.5	0.1158	1.264
0.25	47.5	0.1028	1.221	27.6	0.2929	1.056	39.1	0.2279	1.269
0.3	47.5	0.1463	1.258	27.5	0.3371	1.156	38.6	0.3861	1.323
0.4	46.5	0.2759	1.338	27.4	0.3719	1.221	38.3	0.4494	1.419
0.5	46.5	0.3705	1.421	27.4	0.4197	1.314	38.2	0.5045	1.468

Table 2 The 2nd natural frequencies, resonant responses and damping ratios of three composite plates under different excitation amplitudes

Excitation amplitude (g)	Composite plate *A*			Composite plate *B*			Composite plate *C*		
	Natural frequency (Hz)	Resonant response (m/s)	Damping ratio (%)	Natural frequency (Hz)	Resonant response (m/s)	Damping ratio (%)	Natural frequency (Hz)	Resonant response (m/s)	Damping ratio (%)
0.25	77.0	0.0390	0.683	167.5	0.0703	0.253	89.5	0.0349	0.341
0.75	76.5	0.1076	0.851	167	0.1575	0.434	89.4	0.0785	0.445
1	76.5	0.1665	1.047	165.5	0.1935	0.603	89.2	0.1382	0.487
1.5	76.5	0.1889	1.108	165.6	0.2498	0.605	89.1	0.1629	0.588
2	76.0	0.2560	1.144	164.8	0.3173	0.635	89.0	0.2034	0.644

Journal: 11071 MS: 4486 TYPESET DISK LE CP Disp.:2018/7/31 Pages: 23 Layout: Medium

Table 3 The 3rd natural frequencies, resonant responses and damping ratios of three composite plates under different excitation amplitudes

Excitation amplitude (g)	Composite plate *A*			Composite plate *B*			Composite plate *C*		
	Natural frequency (Hz)	Resonant response (m/s)	Damping ratio (%)	Natural frequency (Hz)	Resonant response (m/s)	Damping ratio (%)	Natural frequency (Hz)	Resonant response (m/s)	Damping ratio (%)
0.2	268.0	0.0070	0.700	187.5	0.0241	0.319	241.2	0.0124	0.421
0.25	267.0	0.0079	0.815	187.3	0.0278	0.346	241.1	0.0158	0.473
0.5	266.5	0.0104	0.833	186.6	0.0434	0.360	240.7	0.0305	0.543
0.75	266.5	0.0176	0.868	186.1	0.0572	0.368	240.2	0.0450	0.593
1	266.0	0.0189	0.885	185.8	0.0724	0.429	240.0	0.0603	0.662

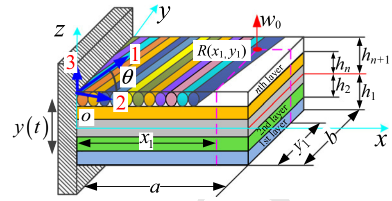

Fig. 6 A theoretical model of fiber-reinforced composite thin plate

parameters which are related to elastic moduli, and C_i and D_i are the nonlinear damping parameters which are related to loss factors of fiber composite. (We will discuss how to obtain these key parameters in Sect. 4.)

The maximum dimensionless strain energy density U_e^{Δ} of fiber-reinforced plate can be expressed as

$$U_e^{\Delta} = \frac{U^{\Delta}}{U_0} \tag{4}$$

where U^{Δ} is the strain energy density, whose expression can be written as $U^{\Delta} = \frac{1}{2abh}\int_0^a\int_0^b\int_0^h \sigma_x\varepsilon_x + \sigma_y\varepsilon_y + \sigma_{xy}\gamma_{xy}\mathrm{d}x\mathrm{d}y$, and $\sigma_x,\ \sigma_y\ \sigma_{xy}$ and $\varepsilon_x,\ \varepsilon_y,\ \gamma_{xy}$ are the stresses and strains in different fiber directions. Besides, U_0 is the constant which is used to make U_e^{Δ} dimensionless, which should have the same power series with U^{Δ}.

Because the composite plate is symmetrical between the middle surface, its inner and outer displacements are decoupled. Then, according to the classical laminate theory, the displacement field can be expressed as

$$\begin{aligned} u(x, y, z, t) &= u_0(x, y, t) - z\frac{\partial w_0(x, y, t)}{\partial x} \\ v(x, y, z, t) &= v_0(x, y, t) - z\frac{\partial w_0(x, y, t)}{\partial y} \\ w(x, y, z, t) &= w_0(x, y, t) \end{aligned} \tag{5}$$

where t is the time, u, v, w represents the displacement of any point of composite plates, and u_0, v_0, w_0 is the displacement in the midplane.

Based on the assumed displacement field of the classical laminate theory, the normal strain ε_z, shear strain γ_{yz} and γ_{xz} of composite plate are equal to zero, i.e., $\varepsilon_z = \gamma_{yz} = \gamma_{xz} = 0$. Then, by considering the relationship between strain and displacement, the strain of any point in the composite plate can be obtained with the following expressions

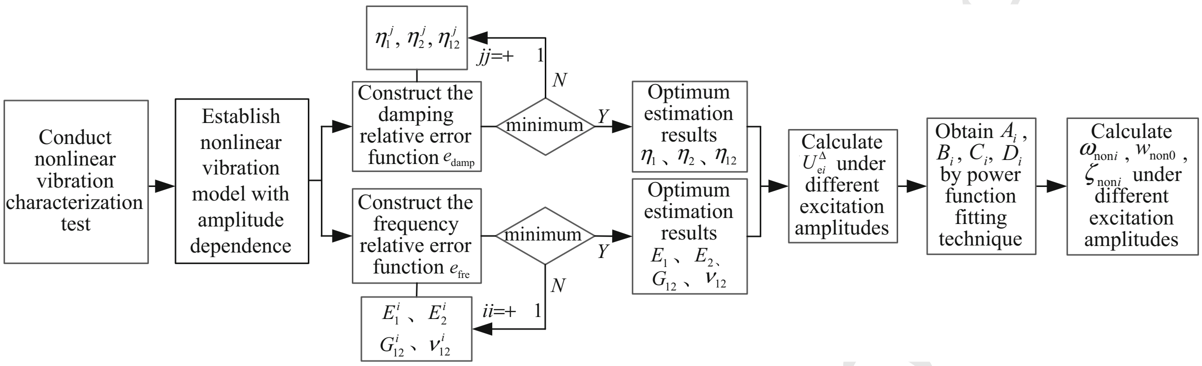

Fig. 7 Calculation flowchart of nonlinear vibration characteristics of fiber-reinforced composite thin plate with amplitude dependence

$$\varepsilon_x = \frac{\partial u}{\partial x} = -z\frac{\partial^2 w_0}{\partial x^2}$$
$$\varepsilon_y = \frac{\partial v}{\partial y} = -z\frac{\partial^2 w_0}{\partial y^2}$$
$$\gamma_{xy} = \frac{\partial u}{\partial y} + \frac{\partial v}{\partial x} = -2z\frac{\partial^2 w_0}{\partial x \partial y} \tag{6}$$

The bending curvatures κ_x , κ_y and torsion curvature κ_{xy} of composite plate on the middle surface can be expressed as

$$\kappa_x = -\frac{\partial^2 w_0}{\partial x^2}, \kappa_y = -\frac{\partial^2 w_0}{\partial y^2}, \kappa_{xy} = -2\frac{\partial^2 w_0}{\partial x \partial y} \tag{7}$$

Then, the strain of any point in the composite plate can be simplified as

$\varepsilon_x = z\kappa_x, \varepsilon_y = z\kappa_y, \gamma_{xy} = z\kappa_{xy}$

For the orthotropic material, the stress–strain relationship in the fiber coordinate can be defined as

$$\begin{Bmatrix} \sigma_1 \\ \sigma_2 \\ \sigma_{12} \end{Bmatrix} = \begin{bmatrix} Q_{11} & Q_{12} & 0 \\ Q_{21} & Q_{22} & 0 \\ 0 & 0 & Q_{66} \end{bmatrix} \begin{Bmatrix} \varepsilon_1 \\ \varepsilon_2 \\ \gamma_{12} \end{Bmatrix} \tag{8}$$

where Q_{ij} is the reduced stiffness, which can be expressed as

$$Q_{11} = \frac{E^*_{\mathrm{non1}}}{1-\nu_{12}\nu_{21}}, \quad Q_{12} = \frac{\nu_{12}E^*_{\mathrm{non2}}}{1-\nu_{12}\nu_{21}}$$
$$Q_{22} = \frac{E^*_{\mathrm{non2}}}{1-\nu_{12}\nu_{21}}, \quad Q_{66} = G^*_{\mathrm{non12}}, \quad \nu_{21} = \nu_{12}\frac{E^*_{\mathrm{non2}}}{E^*_{\mathrm{non1}}} \tag{9}$$

where υ_{12} and υ_{21} are the Poisson's ratio which are induced by the stress in "1" and "2" directions.

When an angle θ exists between the fiber coordinate and global coordinate, the stress–strain relationship of the kth layer of composite plate in the global coordinate

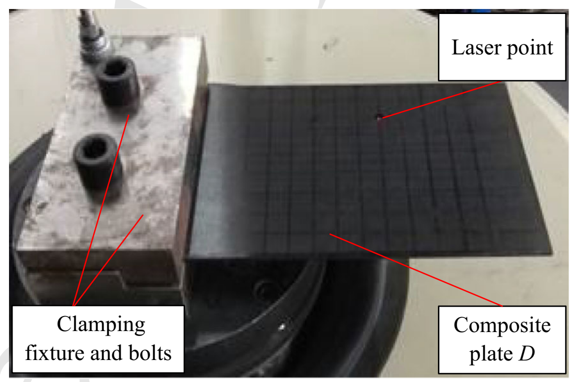

Fig. 8 The real picture of composite plate D

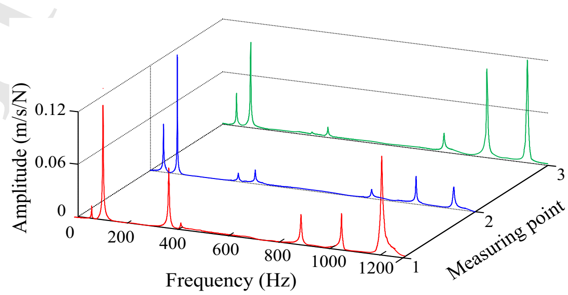

Fig. 9 The measured frequency response functions of composite plate D

can be calculated by using stress–strain transformation equation, which has the following form

$$\begin{Bmatrix} \sigma_x \\ \sigma_y \\ \sigma_{xy} \end{Bmatrix}^{(k)} = \begin{bmatrix} \bar{Q}_{11} & \bar{Q}_{12} & \bar{Q}_{16} \\ \bar{Q}_{12} & \bar{Q}_{22} & \bar{Q}_{26} \\ \bar{Q}_{16} & \bar{Q}_{26} & \bar{Q}_{66} \end{bmatrix}^{(k)} \begin{Bmatrix} \varepsilon_x \\ \varepsilon_y \\ \gamma_{xy} \end{Bmatrix}$$
$$= \begin{bmatrix} \bar{Q}_{11} & \bar{Q}_{12} & \bar{Q}_{16} \\ \bar{Q}_{12} & \bar{Q}_{22} & \bar{Q}_{26} \\ \bar{Q}_{16} & \bar{Q}_{26} & \bar{Q}_{66} \end{bmatrix}^{(k)} \begin{Bmatrix} z\kappa_x \\ z\kappa_y \\ z\kappa_{xy} \end{Bmatrix} \tag{10}$$

Journal: 11071 MS: 4486 TYPESET DISK LE CP Disp.:2018/7/31 Pages: 23 Layout: Medium

Table 4 The first 7 natural frequencies and modal shapes of composite plate D obtained by the experimental test and theoretical calculation

Modal order	Measured natural frequency A (Hz)	Calculated natural frequency B (Hz)	Error $\|B - A\| / A$ (%)	Measured modal shape	Calculated modal shape
1	52.6	54.5	3.6	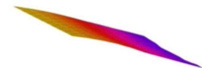	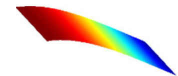
2	106.5	108.3	1.7	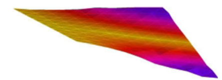	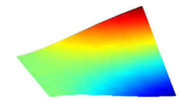
3	325.8	341.6	4.8	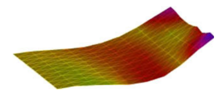	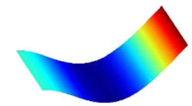
4	409.2	431.7	5.5	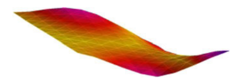	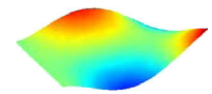
5	881.0	934.7	6.1	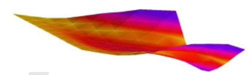	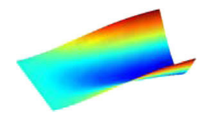
6	1042.0	1065.5	2.3	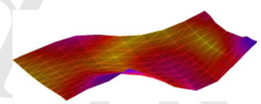	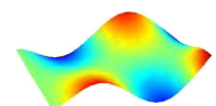
7	1208.0	1277.4	5.7	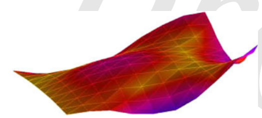	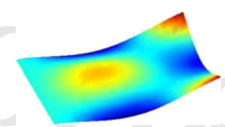

Journal: **11071** MS: **4486** ☐ TYPESET ☐ DISK ☐ LE ☐ CP Disp.:**2018/7/31** Pages: **23** Layout: **Medium**

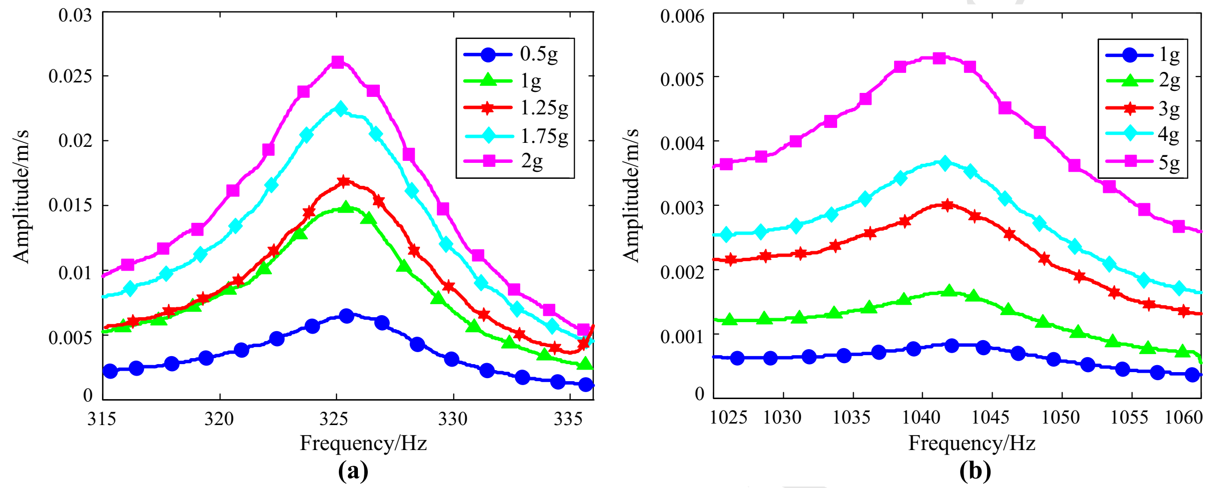

Fig. 10 The measured 3rd and 6th frequency response spectrums of composite plate D under different excitation amplitudes. **a** The 3rd frequency response spectrums. **b** The 6th frequency response spectrums

where $\bar{Q}_{ij}$ is the transformed reduced stiffness, which can be expressed as

$$
\begin{aligned}
\bar{Q}_{11} &= Q_{11}\cos^4\theta_k + 2(Q_{12}+2Q_{66})\sin^2\theta_k \\
&\quad \cos^2\theta_k + Q_{22}\sin^4\theta_k \\
\bar{Q}_{12} &= (Q_{11}+Q_{22}-4Q_{66})\sin^2\theta_k \\
&\quad \cos^2\theta_k + Q_{12}\left(\sin^4\theta_k+\cos^4\theta_k\right) \\
\bar{Q}_{22} &= Q_{11}\sin^4\theta_k + 2\left(Q_{12}+2Q_{66}\right)\sin^2\theta_k \\
&\quad \cos^2\theta_k + Q_{22}\cos^4\theta_k \\
\bar{Q}_{16} &= (Q_{11}-Q_{12}-2Q_{66})\sin\theta_k\cos^3\theta_k \\
&\quad +(Q_{12}-Q_{22}+2Q_{66})\sin^3\theta_k\cos\theta_k \\
\bar{Q}_{26} &= (Q_{11}-Q_{12}-2Q_{66})\sin^3\theta_k \\
&\quad \cos\theta_k + (Q_{12}-Q_{22}+2Q_{66})\sin\theta_k\cos^3\theta_k \\
\bar{Q}_{66} &= (Q_{11}+Q_{22}-2Q_{12}-2Q_{66})\sin^2\theta_k \\
&\quad \cos^2\theta_k + Q_{66}\left(\sin^4\theta_k+\cos^4\theta_k\right)
\end{aligned} \tag{11}
$$

where k represents the kth layer of composite plates and θ_k represents the angle between the fiber direction and the x direction.

The bending and twisting moment resultants in composite plates can be expressed as

$$
\begin{aligned}
\begin{bmatrix} M_x \\ M_y \\ M_{xy} \end{bmatrix} &= \sum_{k=1}^{n}\int_{z_{k-1}}^{z_k}\begin{bmatrix} \sigma_x \\ \sigma_y \\ \sigma_{xy} \end{bmatrix}^{(k)} z\mathrm{d}z \\
&= \sum_{k=1}^{n}\int_{z_{k-1}}^{z_k}\begin{bmatrix} \bar{Q}_{11} & \bar{Q}_{12} & \bar{Q}_{16} \\ \bar{Q}_{12} & \bar{Q}_{22} & \bar{Q}_{26} \\ \bar{Q}_{16} & \bar{Q}_{26} & \bar{Q}_{66} \end{bmatrix}^{(k)} \begin{Bmatrix} z\kappa_x \\ z\kappa_y \\ z\kappa_{xy} \end{Bmatrix} z\mathrm{d}z \\
&= \begin{bmatrix} D_{11} & D_{12} & D_{16} \\ D_{12} & D_{22} & D_{26} \\ D_{16} & D_{26} & D_{66} \end{bmatrix} \begin{Bmatrix} \kappa_x \\ \kappa_y \\ \kappa_{xy} \end{Bmatrix}
\end{aligned} \tag{12}
$$

where,

$$
D_{ij} = \frac{1}{3}\sum_{k=1}^{n}\left(\bar{Q}_{ij}\right)^{(k)}\left(z_k^3 - z_{k-1}^3\right), \quad i,j=1,2,6
$$

The composite plate is subjected to the base excitation load $y\left(t\right)$, which can be expressed as

$$
y\left(t\right) = Ye^{\mathrm{i}\omega t} \tag{13}
$$

where Y is the base excitation amplitude, ω is the excitation frequency, and t is the time.

Assume that the base excitation can be simplified as the external load of uniform inertia force f, which has the following expression

$$
f\left(t\right) = -\rho h\frac{\mathrm{d}^2 y\left(t\right)}{\mathrm{d}t^2} = \rho hY\omega^2 e^{\mathrm{i}\omega t} \tag{14}
$$

Then, the bending strain energy stored in the composite plate can be expressed as

$$
U = \frac{1}{2}\int\int_R \left[M_x\kappa_x + M_y\kappa_y + M_{xy}\kappa_{xy}\right]\mathrm{d}x\mathrm{d}y \tag{15}
$$

The kinetic energy of composite plate can be expressed as

$$
T = \frac{\rho h}{2}\int\int_R \left(\frac{\partial w_0}{\partial t}\right)^2 \mathrm{d}x\mathrm{d}y \tag{16}
$$

The external work done by the uniform inertia force is

$$
W_f = \int\int_R f(t)w_0\mathrm{d}x\mathrm{d}y \tag{17}
$$

Table 5 The 3rd and 6th natural frequencies, resonant responses and damping ratios of composite plate D under different excitation amplitudes

3 Mode				6 Mode			
Excitation amplitude (g)	Natural frequency (Hz)	Resonant response (m/s)	Damping ratio (%)	Excitation amplitude (g)	Natural frequency (Hz)	Resonant response (m/s)	Damping ratio (%)
0.5	325.8	0.0065	0.868	1	1042.0	0.0008	0.972
1	325.6	0.0148	0.874	2	1041.9	0.0016	1.083
1.25	325.5	0.0169	0.898	3	1041.8	0.0030	1.117
1.75	325.4	0.0225	0.984	4	1041.6	0.0037	1.124
2	325.1	0.0261	0.999	5	1041.4	0.0052	1.165

Table 6 The identified elastic moduli and loss factors corresponding to the 6th mode of composite plate under different excitation amplitudes

Excitation amplitude (g)	E_1 (GPa)	E_2 (GPa)	G_{12} (GPa)	η_1	η_2	η_6
1	115.58	9.62	5.24	0.0135	0.0197	0.0251
2	115.56	9.60	5.22	0.0166	0.0207	0.0264
3	115.54	9.58	5.20	0.0167	0.0208	0.0265
4	115.52	9.56	5.18	0.0169	0.0211	0.0269
5	115.52	9.54	5.16	0.0180	0.0213	0.0272

Journal: **11071** MS: **4486** ☐ TYPESET ☐ DISK ☐ LE ☐ CP Disp.:**2018/7/31** Pages: **23** Layout: **Medium**

Table 7 The maximum dimensionless strain energy density values corresponding to the 6th mode of composite plate under different excitation amplitudes

Excitation amplitude (g)	1	2	3	4	5
U_e^{Δ}	5.3	20.9	47.3	84.7	133.6

3.2 Nonlinear vibration solutions

The displacement w_0 of any vibration response point $R(x_1, y_1)$ in the composite plate can be expressed as

$$w_0 = e^{i\omega t} W(\xi, \eta) \tag{18}$$

where ω is the excitation frequency, and $W(\xi, \eta)$ represents modal shape function which can be defined as

$$W(\xi, \eta) = \sum_{i=1}^{M} \sum_{j=1}^{N} q_{ij} P_i(\xi) P_j(\eta) \tag{19}$$

where q_{ij} are the eigenvectors which need to be solved, $P_i(\xi)\,(i = 1, \ldots, M)$ and $P_j(\eta)\,(j = 1, \ldots, N)$ are the orthogonal polynomials.

The orthogonal polynomials can be obtained by implementing orthogonalization operation on polynomial function, which should satisfy the boundary condition of composite plate, and these polynomials have the following expressions

$$\begin{aligned} &P_1(\xi) = \chi(\xi),\ P_1(\eta) = \kappa(\eta) \\ &P_2(\phi) = (\phi - H_2) P_1(\phi) \\ &P_i(\phi) = (\phi - H_i) P_{i-1}(\phi) - V_i P_{i-2}(\phi) \\ &\quad \phi = \xi, \eta, \quad i > 2 \end{aligned} \tag{20}$$

where H_i and V_i are the coefficient functions and their expressions can be written as

$$\begin{aligned} H_i &= \frac{\int_0^1 W(\phi)\left[P_{i-1}(\phi)\right]^2 \phi \mathrm{d}\phi}{\int_0^1 W(\phi)\left[P_{i-1}(\phi)\right]^2 \mathrm{d}\phi} \\ V_i &= \frac{\int_0^1 W(\phi) P_{i-1}(\phi) P_{i-2}(\phi) \phi \mathrm{d}\phi}{\int_0^1 W(\phi)\left[P_{i-2}(\phi)\right]^2 \mathrm{d}\phi}, \phi = \xi, \eta \end{aligned} \tag{21}$$

where $W(\phi)$ is the weighting function and usually $W(\phi) = 1$. Besides, $\chi(\xi)$ and $\kappa(\eta)$ are the polynomial functions which should satisfy the different boundary conditions, such as the clamped, simply support and free boundary. These functions can be expressed as

$$\chi(\xi) = \xi^{\alpha}(1-\xi)^{\beta}, \quad \kappa(\eta) = \eta^{\gamma}(1-\eta)^{\tau}$$

$$\xi = x/a, \quad \eta = y/b \tag{22}$$

As the studied composite plate is under the cantilever boundary condition, the corresponding values can be set as $\alpha = 2$, $\beta = 0$, $\gamma = 0$, $\tau = 0$. Then, substituting Eq. (19) into Eqs. (15)–(17), the maximum bending strain energy $U_{\max}$ stored in the plate, the maximum kinetic energy $T_{\max}$ and the maximum external work $W_{f\max}$ done by the uniform inertia force can be obtained and expressed as

$$\begin{aligned} U_{\max} = \frac{1}{2} \int\int_R \Bigg[& D_{11}\left(\frac{\partial^2 W}{\partial x^2}\right)^2 + 2D_{12}\frac{\partial^2 W}{\partial x^2}\frac{\partial^2 W}{\partial y^2} \\ & + D_{22}\left(\frac{\partial^2 W}{\partial y^2}\right)^2 \\ & + 4\left(D_{16}\frac{\partial^2 W}{\partial x^2} + D_{26}\frac{\partial^2 W}{\partial y^2}\right)\frac{\partial^2 W}{\partial x \partial y} \\ & + 4D_{66}\left(\frac{\partial^2 W}{\partial x \partial y}\right)^2 \Bigg] \mathrm{d}x\mathrm{d}y \end{aligned} \tag{23}$$

$$T_{\max} = \frac{\rho h \omega^2}{2} \int\int_R (W)^2 \mathrm{d}x\mathrm{d}y \tag{24}$$

$$W_{f\max} = \rho h Y \omega^2 \int\int_R W \mathrm{d}x\mathrm{d}y \tag{25}$$

Define the Lagrangian energy function L as

$$L = T_{\max} + W_{f\max} - U_{\max} \tag{26}$$

By minimizing partial derivative of the Lagrangian energy function L with respect to q_{ij} in the following equation

$$\frac{\partial L}{\partial q_{ij}} = 0, i = 1, 2, \ldots, M,\ j = 1, 2, \ldots, N. \tag{27}$$

Then, $M \times N$ equations in frequency domain can be obtained and written as the matrix form, and the vibration equation of composite thin plate with the consideration of amplitude-dependent nonlinear effects can be expressed as

$$\left(\boldsymbol{K}_{\mathrm{non}}^{*} - \omega^2 \boldsymbol{M}\right)\boldsymbol{q} = \boldsymbol{F} \tag{28}$$

where $\boldsymbol{K}_{\mathrm{non}}^{*}$ is complex nonlinear stiffness matrix which can be rewritten as $\boldsymbol{K}_{\mathrm{non}} + \mathrm{i}\boldsymbol{C}_{\mathrm{non}}$, and $\boldsymbol{K}_{\mathrm{non}}$, $\boldsymbol{C}_{\mathrm{non}}$ and $\boldsymbol{M}$ are the nonlinear stiffness matrix, nonlinear material damping matrix and mass matrix, respectively. Besides, $\boldsymbol{q} = (q_{11}, q_{12}, \ldots q_{ij})^{\mathrm{T}}$ is the response vector and $\boldsymbol{F}$ is

Journal: 11071 MS: 4486 ☐ TYPESET ☐ DISK ☐ LE ☐ CP Disp.:2018/7/31 Pages: 23 Layout: Medium

exciting force vector. It should be noted that the nonlinear vibration equation can be converted to the linear vibration equation with ignoring A_i , B_i , C_i and D_i, which has the following form

$$\left(\boldsymbol{K}^{*}-\omega^{2}\boldsymbol{M}\right)\boldsymbol{q}=\boldsymbol{F} \tag{29}$$

where $\boldsymbol{K}^{*}$ is the complex linear stiffness matrix without considering the amplitude-dependent nonlinearity.

Ignoring the damping matrix and the exciting force vector in Eq. (28), the free vibration eigenvalue equation of composite thin plate with considering amplitude-dependent nonlinearity can be obtained and written as

$$\left(\boldsymbol{K}_{\text{non}}-\omega^{2}\boldsymbol{M}\right)\boldsymbol{q}=0 \tag{30}$$

In order to make Eq. (30) have the nonzero solution or nontrivial solution, the determinant of the coefficient matrix should be equal to zero

$$\left|\boldsymbol{K}_{\text{non}}-\omega_i^{2}\boldsymbol{M}\right|=0 \tag{31}$$

In order to solve nonlinear natural frequencies of composite plate, the iteration technique is employed to solve Eq. (31) when the iteration initial value $\omega_i^{(0)}$ is determined. Besides, according to the minimum difference principle of the two adjacent natural frequency results, the iteration termination condition can be expressed as

$$\left|\omega_i^{(j+1)}-\omega_i^{(j)}\right|\leq S_0 \tag{32}$$

where S_0 is the iteration accuracy factor, $\omega_i^{(j)}$ is the jth step of natural frequency results, $\omega_i^{(j+1)}$ is the j+1th step of natural frequency results (superscript j or j+1 represents the different iteration calculation steps).

By solving Eq. (32) with iterative optimization techniques [27,28], the ith nonlinear natural frequency $\omega_{\text{non}i}$ of composite plate can be determined. Then, the Newton–Raphson iteration method can be used to calculate the nonlinear vibration response. The expression of residual vector $\boldsymbol{r}$ can also be derived and expressed as follows

$$\boldsymbol{r}=\left(\boldsymbol{K}_{\text{non}}^{*}-\omega^{2}\boldsymbol{M}\right)\boldsymbol{q}-\boldsymbol{F} \tag{33}$$

Because $\boldsymbol{r}$ is a complex vector which includes the real part $\boldsymbol{q}_{\text{R}}$ and imaginary part $\boldsymbol{q}_{\text{I}}$ of the response vector $\boldsymbol{q}$, it can be written in the form of $\boldsymbol{q}_{\text{R}}+\text{i}\boldsymbol{q}_{\text{I}}$. Then, the Jacobian matrix $\boldsymbol{J}$ related to $\boldsymbol{r}$ can be expressed as

$$\boldsymbol{J}=\begin{bmatrix}\text{R}(\partial\boldsymbol{r}/\partial\boldsymbol{q}_{\text{R}}) & \text{R}(\partial\boldsymbol{r}/\partial\boldsymbol{q}_{\text{I}})\\ \text{I}(\partial\boldsymbol{r}/\partial\boldsymbol{q}_{\text{R}}) & \text{I}(\partial\boldsymbol{r}/\partial\boldsymbol{q}_{\text{I}})\end{bmatrix} \tag{34}$$

$$\frac{\partial\boldsymbol{r}}{\partial\boldsymbol{q}_{\text{R}}}=\boldsymbol{K}_{\text{non}}^{*}-\omega^{2}\boldsymbol{M} \tag{35}$$

$$\frac{\partial\boldsymbol{r}}{\partial\boldsymbol{q}_{\text{I}}}=\text{i}(\boldsymbol{K}_{\text{non}}^{*}-\omega^{2}\boldsymbol{M}) \tag{36}$$

Meanwhile, by separating the real and imaginary parts of the residual vector $\boldsymbol{r}$ and the response vector $\boldsymbol{q}$, the separation vectors of $\bar{\boldsymbol{r}}$ and $\bar{\boldsymbol{q}}$ can be obtained and expressed as

$$\bar{\boldsymbol{r}}=\begin{Bmatrix}\text{R}(\boldsymbol{r})\\ \text{I}(\boldsymbol{r})\end{Bmatrix} \tag{37}$$

$$\bar{\boldsymbol{q}}=\begin{Bmatrix}\text{R}(\boldsymbol{q})\\ \text{I}(\boldsymbol{q})\end{Bmatrix} \tag{38}$$

By combining with Eq. (34)–(38), the Newton–Raphson iteration formula of Eq. (33) can be expressed as

$$\bar{\boldsymbol{r}}^{(j)}+\boldsymbol{J}^{(j)}\times\Delta\bar{\boldsymbol{q}}^{(j)}=0 \tag{39a}$$

$$\bar{\boldsymbol{q}}^{(j+1)}=\bar{\boldsymbol{q}}^{(j)}+\Delta\bar{\boldsymbol{q}}^{(j)} \tag{39b}$$

$$\boldsymbol{q}^{(j+1)}=\text{R}(\bar{\boldsymbol{q}}^{(j+1)})+\text{i}\times\text{I}(\bar{\boldsymbol{q}}^{(j+1)}) \tag{39c}$$

where $\Delta\bar{\boldsymbol{q}}^{(j)}$ represents the response increment at the jth step (superscript j or j+1 represents the different iteration calculation steps).

Then, substituting the iteration initial value of resonant response $\boldsymbol{q}^{(0)}$(when $j=0$) into Eq. (39), the iteration termination condition can be determined by setting 2-norm of residual vector $\boldsymbol{r}$ less than the iteration accuracy factor S_0 (e.g., set $S_0=0.0001$), which has the following form

$$\left\|\boldsymbol{r}^{(j+1)}\right\|_2=\sqrt{\left(\left|r_1^{(j+1)}\right|^2+\left|r_2^{(j+1)}\right|^2+\left|r_3^{(j+1)}\right|^2+\ldots\right)}\leq S_0 \tag{40}$$

When the 2-norm of residual vector $\boldsymbol{r}$ in Eq. (39b) satisfies the iteration termination condition, the response vector $\boldsymbol{q}$ can also be obtained using Eq. (39). Further, by substituting $\boldsymbol{q}$ into Eq. (18), the nonlinear vibration response $w_{\text{non}0}$ of composite plate under a certain exciting frequency can be obtained.

Once the nonlinear vibration response $w_{\text{non}0}$ is acquired, the total strain energy of composite plate U and the strain energy U_1 , U_2 and U_{12} in different fiber directions can be calculated and expressed as

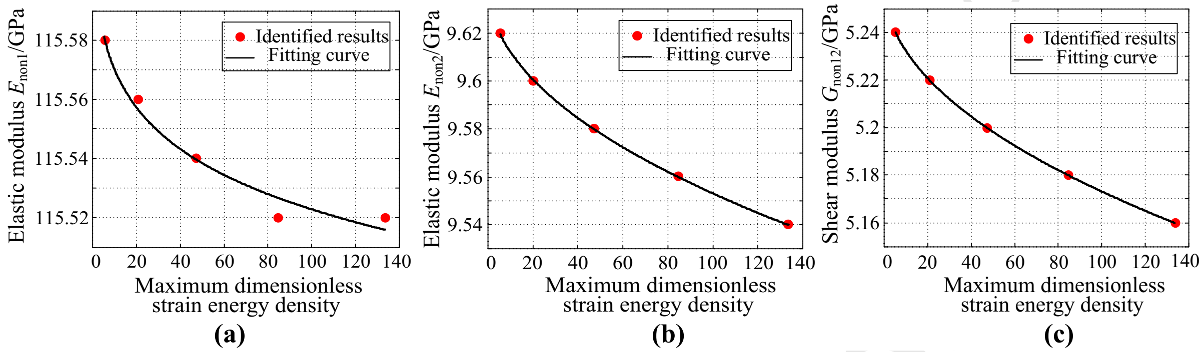

Fig. 11 The identified relation curves between elastic moduli and the maximum dimensionless strain energy density along the longitudinal, transverse and shear directions of fiber-reinforced composite. **a** The longitudinal direction. **b** The transverse direction. **c** The shear direction

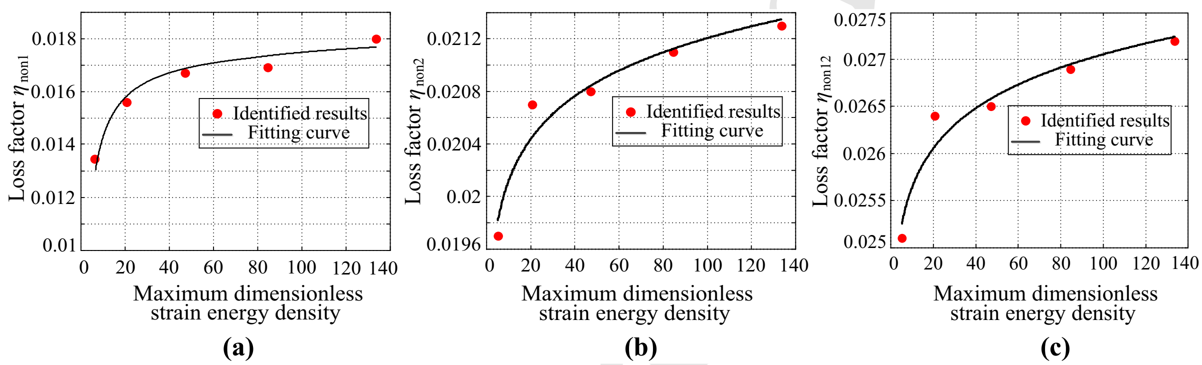

Fig. 12 The identified relation curves between loss factors and the maximum dimensionless strain energy density along the longitudinal, transverse and shear directions of fiber-reinforced composite. **a** The longitudinal direction. **b** The transverse direction. **c** The shear direction

$$
\begin{aligned}
U_1 &= \sum_{k=1}^{n} \frac{1}{2} \int_{x=0}^{a} \int_{y=0}^{b} \int_{h_{k-1}}^{h_k} \sigma_1^k \varepsilon_1^k \mathrm{d}x\mathrm{d}y\mathrm{d}z \\
U_2 &= \sum_{k=1}^{n} \frac{1}{2} \int_{x=0}^{a} \int_{y=0}^{b} \int_{h_{k-1}}^{h_k} \sigma_2^k \varepsilon_2^k \mathrm{d}x\mathrm{d}y\mathrm{d}z \\
U_{12} &= \sum_{k=1}^{n} \frac{1}{2} \int_{x=0}^{a} \int_{y=0}^{b} \int_{h_{k-1}}^{h_k} \tau_{12}^k \gamma_{12}^k \mathrm{d}x\mathrm{d}y\mathrm{d}z \\
U &= U_1 + U_2 + U_{12}
\end{aligned} \tag{41}
$$

Next, on the basis of modal strain energy method, the relationship between modal loss factors and loss factors in different fiber directions can be expressed as

$$
\eta_{\mathrm{non}i} = \frac{\eta_{\mathrm{non1}} U_1 + \eta_{\mathrm{non2}} U_2 + \eta_{\mathrm{non12}} U_{12}}{U} \tag{42}
$$

Finally, the nonlinear modal damping ratio $\zeta_{\mathrm{non}i}$, which is often used in engineering practice, can be obtained as

$$
\zeta_{\mathrm{non}i} = \frac{\eta_{\mathrm{non}i}}{2} \tag{43}
$$

4 Determination of the nonlinear stiffness and damping parameters

In this section, the principle of how to determine the key stiffness and damping parameters in the proposed nonlinear vibration model, such as A_i, B_i, C_i and D_i, is illustrated.

4.1 Identify the elastic moduli and loss factors without considering amplitude dependence

Firstly, by using the least square method, the frequency relative error function e_{fre} between the experimental

Journal: 11071 MS: 4486 TYPESET DISK LE CP Disp.:2018/7/31 Pages: 23 Layout: Medium

natural frequencies and the theoretical natural frequencies can be constructed under a certain excitation amplitude, which can be obtained by solving Eq. (29) with the following expression

$$e_{\text{fre}} = \sum_{i=1}^{R_{\text{mode}}} \left(\frac{|\Delta f_i|}{\hat{f}_i} \right)^2 \tag{44}$$

where R_{mode} represents the number of modes, Δf_i represents the difference between the ith natural frequency obtained by the experiment and theoretical calculation, $\hat{f}_i$ is the ith natural frequency obtained in the experiment.

Then, take the average material parameters as the center, such as E_1^0, E_2^0, G_{12}^0, ν_{12}^0, which are usually provided by composite material manufacturer. With the consideration of parameters error $R_{\text{err}} = 10\text{–}\sim 20\%$, the range of elastic moduli can be determined as follows

$$\begin{aligned} &E_1^0\,(1 - R_{\text{err}}) \le E_1 \le E_1^0\,(1 + R_{\text{err}}) \\ &E_2^0\,(1 - R_{\text{err}}) \le E_2 \le E_2^0\,(1 + R_{\text{err}}) \\ &G_{12}^0\,(1 - R_{\text{err}}) \le G_{12} \le G_{12}^0\,(1 + R_{\text{err}}) \end{aligned} \tag{45}$$

Further, select an appropriate step size g (for example g=1%) in the above range and construct the iteration vectors of the elastic moduli, such as $\boldsymbol{E}_1, \boldsymbol{E}_2, \boldsymbol{G}_{12}$, which can be expressed as

$$\boldsymbol{Z} = [Z^1, Z^2, \ldots Z^n] \tag{46}$$

where $Z^1 = Z^0(1 - R_{\text{err}})$, $Z^2 = Z^0(1 - R_{\text{err}}) + 2gR_{\text{err}}Z^0$, $Z^n = Z^0(1 - R_{\text{err}}) + 2g(n-1)R_{\text{err}}Z^0$, $Z = E_1, E_2, G_{12}$.

By iteratively calculating these material parameters in a permutation and combination manner, the optimum estimation results of E_1, E_2, G_{12} without considering amplitude dependence under certain excitation amplitude can be obtained when e_{fre} reaches the minimum value. Consequently, by repeating the above steps, the elastic moduli in different fiber directions under different excitation amplitudes can be identified.

Similarly, the damping relative error function e_{damp} can be constructed and expressed as

$$e_{\text{damp}} = \sum_{r=1}^{R_{\text{mode}}} \left(\frac{|\Delta \zeta_i|}{\left|\hat{\zeta}_i\right|} \right)^2 \tag{47}$$

where $\Delta\zeta_i$ represents the difference between the ith modal damping ratio obtained by the experiment and theoretical calculation and $\hat{\zeta}_i$ is the ith modal damping ratio obtained in the experiment.

Next, set the maximum loss factor, e.g., $\eta_{\max} = 0.04$ (which is large enough for the fiber material), and construct the iteration vectors of loss factors, such as $\boldsymbol{\eta}_1$, $\boldsymbol{\eta}_2$ and $\boldsymbol{\eta}_{12}$ with an appropriate step size g (for example g=1%) in a range of $0 \sim, l\eta_{\max}$, which can be expressed as

$$\begin{aligned} \boldsymbol{\eta}_1 &= \left[\eta_1^1 \quad \eta_1^2 \ldots \ \eta_1^n\right] \\ \boldsymbol{\eta}_2 &= \left[\eta_2^1 \quad \eta_2^2 \ldots \ \eta_2^n\right] \\ \boldsymbol{\eta}_{12} &= \left[\eta_{12}^1 \quad \eta_{12}^2 \ldots \ \eta_{12}^n\right] \end{aligned} \tag{48}$$

where $\eta_i^1 = 0$, $\eta_i^2 = g\eta, \ldots, \eta_i^n = (n-1)g\eta_{\max}$.

By iteratively calculating the loss factors in a permutation and combination manner, the optimum estimation results of η_1, η_2 and η_{12} without considering amplitude dependence under certain excitation amplitude can be obtained when the damping relative error function e_{damp} gets to the minimum value. Finally, by repeating the above steps, the loss factors in different fiber directions under different excitation amplitudes can be identified.

4.2 Determine the maximum dimensionless strain energy density

In this step, the maximum dimensionless strain energy density values are calculated under different excitation amplitudes so as to determine the nonlinear stiffness and damping parameters in the nonlinear vibration model. First, substitute the identified elastic moduli, loss factors and natural frequency under a certain excitation amplitude into Eq. (29) to obtain the response vector $\boldsymbol{q}$ of composite plate. Then, substitute response vector $\boldsymbol{q}$ into Eq. (18) to obtain the displacement w_0. The strain energy density U^{Δ} can also be calculated by substituting w_0 into Eq. (15). Finally, by considering the expression of dimensionless strain energy density in Eq. (4), the maximum dimensionless strain energy density U_{ei}^{Δ} under a certain excitation amplitude can be calculated. And by repeating the above steps, the maximum dimensionless strain energy density values under different excitation amplitudes can be determined.

4.3 Obtain nonlinear parameters by the power function fitting technique

In this step, firstly set the maximum dimensionless strain energy density value as X-axis, while set each of

Journal: 11071 MS: 4486 TYPESET DISK LE CP Disp.:2018/7/31 Pages: 23 Layout: Medium

Table 8 The identified elastic moduli and loss factors of fiber-reinforced composite without considering amplitude dependence

Name	E_1 (GPa)	E_2 (GPa)	G_{12} (GPa)	η_1	η_2	η_{12}
Linear material parameter	115.70	9.64	5.26	0.0126	0.0171	0.0236

Table 9 The identified nonlinear stiffness and damping parameters of fiber-reinforced composite with considering amplitude dependence

Name	Longitudinal direction		Transverse direction		Shear direction	
Nonlinear material parameter	A_1	− 0.000980	A_2	− 0.000983	A_{12}	−0.001801
	B_1	0.11971	B_2	0.48410	B_{12}	0.48410
	C_1	− 1.33692	C_2	4.66192	C_{12}	4.81225
	D_1	− 0.67641	D_2	0.02747	D_{12}	0.02787

elastic modulus and loss factor as Y-axis, and therefore the relation curve between the X-axis and Y-axis can be plotted. Then, the concerned stiffness and damping parameters in the nonlinear vibration model, such as A_i, B_i, C_i and D_i, can be obtained by the power function fitting technique, which is realized by the curve fitting tool in MATLAB (enter cftool at the command line). Finally, by referring to the following calculation flow chart of fiber-reinforced composite thin plate with amplitude-dependent property, as shown in Fig. 7, the nonlinear natural frequencies, vibration responses and modal damping ratios under different excitation amplitudes can be calculated by the self-written MATLAB program.

5 A case study

In this section, another TC300 carbon/epoxy composite plate, namely composite plate D, is taken as a research object to verify the practicability and reliability of the proposed model.

5.1 Test object

The composite plate D is symmetrically laid with laminate configuration of $[(0/90)_5/0/(90/0)_5]$, as shown in Fig. 8. It has in total 21 layers, and each layer has the same thickness and fiber volume fraction. The longitudinal elastic modulus is 115.7 GPa, transverse elastic modulus is 9.64 GPa, shear modulus is 5.26 GPa, Poisson's ratio is 0.33, and density is 1780 kg/m^3. Besides, the length, width and thickness of the plate D after the clamping are $200 \times 130 \times 2.36$ mm. The laser measuring point is 140 mm above the constraint end, and the horizontal distance between this point and the left free edge of the plate is 20 mm.

5.2 Linear vibration measurement

Based on the same vibration test instruments used in Sect. 2, a modal hammer is added in the linear vibration measurement to conduct the experimental modal test of composite plate D. The frequency response functions are measured with the changes of the excitation positions, and totally 100 measuring points are excited by the hammer. Figure 9 shows the measured frequency response functions at three different excitation points, and Table 4 lists the identified natural frequency and modal shape results. Besides, for the convenience of comparison, the calculated results of the composite plate D are also listed in the same table, from which we can see that there is a good agreement between the calculated and measured modal shapes, and the maximum calculation error of natural frequencies is less than 6.1%.

5.3 Nonlinear vibration measurement

Nonlinear vibration measurement of composite plate D under different excitation amplitudes is taken. By taking the 3rd and 6th modes as an example, firstly set the excitation energy as five different excitation values and

Journal: **11071** MS: **4486** TYPESET DISK LE CP Disp.:**2018/7/31** Pages: **23** Layout: **Medium**

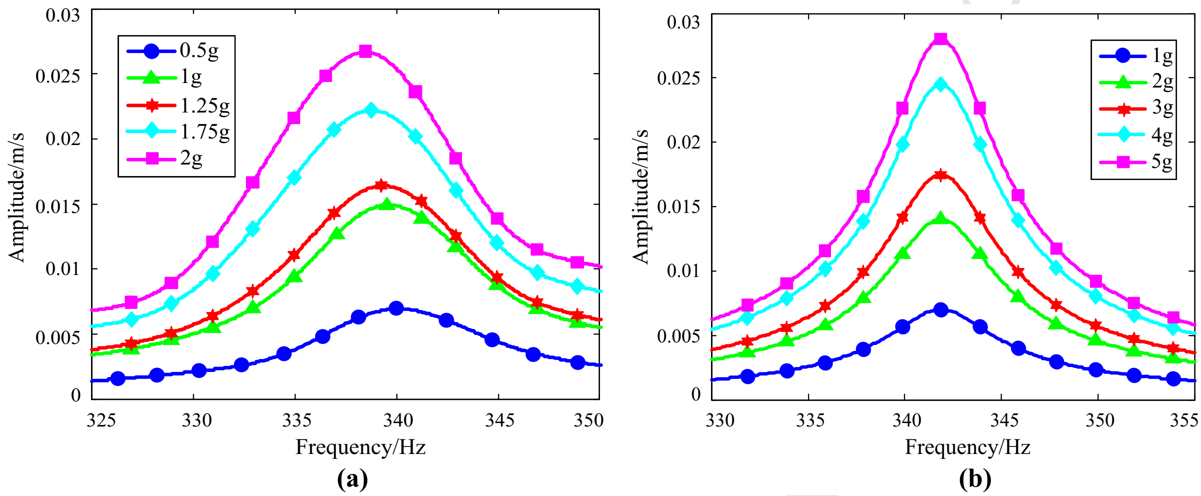

Fig. 13 The 3rd frequency response spectrums of composite plate *D* calculated under different excitation amplitudes. **a** With considering the amplitude-dependent property. **b** Without considering the amplitude-dependent property

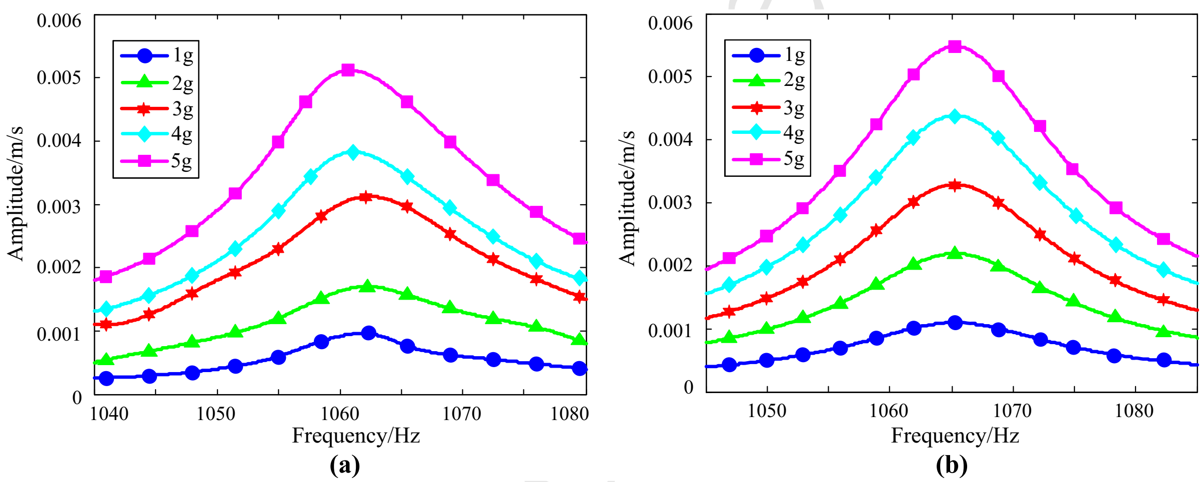

Fig. 14 The 6th frequency response spectrums of composite plate *D* calculated under different excitation amplitudes. **a** With considering the amplitude-dependent property. **b** Without considering the amplitude-dependent property

measure the corresponding frequency response spectrums under different excitation amplitudes, as shown in Fig. 10. Then, the natural frequencies, resonant responses and damping ratios are identified, as listed in Table 5.

5.4 Identification results under different excitation amplitudes

Here, the 6th natural frequency and modal damping results obtained in the above are utilized to calculate elastic moduli, loss factors and the maximum dimensionless strain energy density values under the excitation amplitudes of 1, 2, 3, 4 and 5g, and the identified results are listed in Tables 6 and 7.

5.5 Fitting of the nonlinear stiffness and damping parameters

Since the elastic moduli and loss factors along the longitudinal, transverse and shear directions of the fiber-reinforced composite are already obtained, each of

Table 10 The comparison of the 3rd natural frequencies, resonant responses and damping ratios of composite plate D without considering amplitude dependence

Excitation amplitude (g)	Measured result			Calculated result without considering amplitude dependence					
	Natural fre-quency (Hz) A	Resonant response (m/s) B	Damping ratio (%) C	Natural fre-quency (Hz) D	Resonant response (m/s) E	Damping ratio (%) F	Frequency error $\|D\text{-}A\|/A$ (%)	Response error $\|E\text{-}B\|/B$ (%)	Damping ratio error $\|F\text{-}C\|/C$ (%)
0.5	325.8	0.0065	0.868	341.9	0.0070	0.884	4.9	7.7	1.8
1	325.6	0.0148	0.874	341.9	0.0140	0.884	5.0	5.4	1.1
1.25	325.5	0.0169	0.898	341.9	0.0175	0.884	5.0	3.6	1.6
1.75	325.4	0.0225	0.984	341.9	0.0245	0.884	5.1	8.9	10.2
2	325.1	0.0261	0.999	341.9	0.0280	0.884	5.2	7.3	11.5

Table 11 The comparison of the 3rd natural frequencies, resonant responses and damping ratios of composite plate D with considering amplitude dependence

Excitation amplitude (g)	Measured result			Calculated result with considering amplitude dependence					
	Natural fre-quency (Hz) A	Resonant response (m/s) B	Damping ratio (%) C	Natural fre-quency (Hz) D	Resonant response (m/s) E	Damping ratio (%) F	Frequency error $\|D\text{-}A\|/A$ (%)	Response error $\|E\text{-}B\|/B$ (%)	Damping ratio error $\|F\text{-}C\|/C$ (%)
0.5	325.8	0.0065	0.868	339.7	0.0069	0.861	4.3	6.2	0.8
1	325.6	0.0148	0.874	339.4	0.0149	0.879	4.2	0.7	0.6
1.25	325.5	0.0169	0.898	339.2	0.0164	0.899	4.2	3.0	0.1
1.75	325.4	0.0225	0.984	338.9	0.0222	0.903	4.1	1.3	8.2
2	325.1	0.0261	0.999	338.8	0.0266	0.938	4.2	1.9	6.1

Journal: 11071 MS: 4486 TYPESET DISK LE CP Disp.:2018/7/31 Pages: 23 Layout: Medium

them is used as the dependent variable while the maximum dimensionless strain energy density value is set as the independent variable. Then, the nonlinear relation curves between these variables are obtained by the power function fitting technique, as shown in Fig. 11 and Fig. 12. In addition, the following parameters, such as $E_1, E_2, G_{12}, \eta_1, \eta_2, \eta_{12}, A_i, B_i, C_i$ and D_i in Eq. (1), Eq. (2) and Eq. (3), with and without considering the effect of the amplitude dependence are also identified, as listed in Tables 8 and 9.

5.6 Comparison and discussion

Finally, the identified nonlinear material parameters are brought into the nonlinear vibration model, and therefore the nonlinear natural frequencies, resonant responses, damping ratios and response spectrums in the 3rd and 6th modes of composite plate D under different excitation amplitudes are calculated by the self-written MATLAB program, as given in Fig. 13 to Fig. 14 and Tables 9, 10, 11, 12, and 13. For the convenience of comparison with experimental results, the corresponding calculated results in the 3rd and 6th modes without considering the amplitude dependence are also given in the same figures and tables.

It can be seen from the above results that: (I) For the 3rd mode of composite plate, the maximum calculation errors of natural frequencies, resonant responses and damping ratios with considering amplitude-dependent property are less than 4.3, 6.2 and 8.2%, and these calculation errors are smaller than those obtained without considering the amplitude dependence (which are less than 5.2, 8.9 and 11.5%, respectively); (II) for the 6th mode of composite plate, the maximum calculation errors of natural frequencies, resonant responses and damping ratios with considering amplitude-dependent property are less than 2.1, 12.5 and 9.6%, and these calculation errors are also smaller than those obtained without considering the amplitude dependence (which are less than 2.3, 37.5 and 16.7%, respectively). Therefore, the correctness and effectiveness of the proposed nonlinear vibration model have been verified. However, it is still necessary to find out the reasons for the above errors, which probably result from both theoretical modeling and experimental measurement. For example, in the theoretical modeling process, the following calculation errors exist: (I) without considering the damping effects resulting from interface defects

Table 12 The comparison of the 6th natural frequencies, resonant responses and damping ratios of composite plate D without considering amplitude dependence

Excitation amplitude (g)	Measured result			Calculated result without considering amplitude dependence			Frequency error	Response error	Damping ratio error
	Natural frequency (Hz) A	Resonant response (m/s) B	Damping ratio (%) C	Natural frequency (Hz) D	Resonant response (m/s) E	Damping ratio (%) F	$\lvert D\text{-}A\rvert/A$ (%)	$\lvert E\text{-}B\rvert/B$ (%)	$\lvert F\text{-}C\rvert/C$ (%)
1	1042.0	0.0008	0.972	1065.5	0.0011	1.134	2.3	37.5	16.7
2	1041.9	0.0017	1.083	1065.5	0.0022	1.134	2.3	29.3	4.7
3	1041.8	0.0030	1.117	1065.5	0.0033	1.134	2.3	10.0	1.5
4	1041.6	0.0037	1.124	1065.5	0.0043	1.134	2.3	18.9	0.9
5	1041.4	0.0052	1.165	1065.5	0.0055	1.134	2.3	5.8	2.7

Table 13 The comparison of the 6th natural frequencies, resonant responses and damping ratios of composite plate D with considering amplitude dependence

Excitation amplitude (g)	Measured result			Calculated result with considering amplitude dependence					
	Natural frequency (Hz) A	Resonant response (m/s) B	Damping ratio (%) C	Natural frequency (Hz) D	Resonant response (m/s) E	Damping ratio (%) F	Frequency error $\lvert D\text{-}A\rvert/A$ (%)	Response error $\lvert E\text{-}B\rvert/B$ (%)	Damping ratio error $\lvert F\text{-}C\rvert/C$ (%)
1	1042.0	0.0008	0.972	1063.7	0.0009	0.879	2.1	12.5	9.6
2	1041.9	0.0016	1.083	1062.5	0.0017	1.034	2.0	6.2	4.5
3	1041.8	0.0030	1.117	1061.3	0.0031	1.113	1.9	3.3	0.4
4	1041.6	0.0037	1.124	1060.2	0.0036	1.116	1.8	2.7	0.7
5	1041.4	0.0052	1.165	1059.1	0.0050	1.150	1.7	3.8	1.3

and interfacial frictions between the layers; (II) without considering the effect of residual stress; (III) without considering the influence of the dispersion of composite materials; (IV) without considering the accumulation of the truncation errors and rounding errors in the calculation process. While in the experimental measurement, the following factors may also lead to some errors: (I) without considering the influence of the looseness in the clamped boundary condition; (II) without considering calibration errors of the accelerometer and laser Doppler vibrometer; (III) without considering the influence of air damping.

Finally, after the further analysis and comparison, we can also find out that: (I) The calculated and measured natural frequencies in the 3rd and 6th mode of composite plate decrease with the increase in excitation amplitudes, which all show the soft nonlinear stiffness characteristics. The reason for this phenomenon may be the nonlinear viscoelastic effect of epoxy resin materials, which contributes to frequency and amplitude dependences [29,30]; (II) the calculated damping results show the same trend of enlargement with the measured damping results when the excitation amplitudes increase monotonously, which may be caused by the increased interfacial friction, resulting from the increased response amplitudes [3,4].

6 Conclusions

By combining theory with practice, this research investigates the nonlinear vibration modeling method of composite plate structures with amplitude dependence.

(1) The nonlinear natural frequencies, resonant responses and damping ratios of three different TC300 carbon/epoxy composite plates have been measured in the nonlinear vibration characterization experiment. Based on the measured results under different excitation amplitudes, the nonlinear stiffness and damping phenomena have been observed and confirmed.
(2) A new nonlinear vibration model of fiber-reinforced composite thin plate with amplitude-dependent property has been established based on the Jones–Nelson material nonlinear model. Both of the nonlinear stiffness and damping are considered by expressing the elastic moduli and loss factors of as the function of strain energy density. Then, by combining with the measured natural frequency and

Journal: 11071 MS: 4486 TYPESET DISK LE CP Disp.:2018/7/31 Pages: 23 Layout: Medium

damping data, the power function fitting technique is provided to determine the nonlinear stiffness and damping parameters in this new model.

(3) Another TC300 carbon/epoxy composite plate is taken as study object to verify the practicability and reliability of the proposed model with consideration of more modes and measuring points, and the comparisons between the theoretical and experimental results show a good agreement. Also, it has been proved that the proposed model can provide a reasonable explanation why the composite plate structure shows the soft nonlinear stiffness characteristics and nonlinear damping variation when the excitation amplitudes change.

Acknowledgements This study was supported by the National Natural Science Foundation of China granted No. 51505070, the Fundamental Research Funds for the Central Universities of China granted No. N150304011, N160313002 and N160312001, the Scholarship Fund of China Scholarship Council (CSC) granted No. 201806085032, and the Key Laboratory of Vibration and Control of Aero-Propulsion System Ministry of Education, Northeastern University, granted No.VCAME201603.

Compliance with ethical standards

Conflict of interest The authors declared no potential conflicts of interest with respect to the research, authorship, and/or publication of this article.

References

1. Mallick, P.K.: Fiber-reinforced composites: materials, manufacturing, and design[M]. The Chemical Rubber Company Press, Boca Raton (2007)
2. Gibson, R.F., Plunkett, R.: Dynamic mechanical behavior of fiber-reinforced composites: measurement and analysis. J. Compos. Mater. **10**(4), 325–341 (1976)
3. Chandra, R., Singh, S.P., Gupta, K.: Damping studies in fiber-reinforced composites-a review. Compos. Struct. **46**(1), 41–51 (1999)
4. Yan, L., Jenkins, C.H., Pendleton, R.L.: Polyolefin fiber-reinforced concrete composites: part I. Damping and frequency characteristics. Cem. Concr. Res. **30**(3), 391–401 (2000)
5. Wang, Z.X., Shen, H.S.: Nonlinear vibration and bending of sandwich plates with nanotube-reinforced composite face sheets. Compos. B Eng. **43**(2), 411–421 (2012)
6. Rao, B.N., Pillai, S.R.R.: Non-linear vibrations of a simply supported rectangular antisymmetric cross-ply plate with immovable edges. J. Sound Vib. **152**(3), 568–572 (1992)
7. Singh, G., Rao, G.V., Iyengar, N.G.R.: Non-linear forced vibrations of antisymmetric rectangular cross-ply plates. Compos. Struct. **20**(3), 185–194 (1992)
8. Ribeiro, P., Petyt, M.: Non-linear vibration of composite laminated plates by the hierarchical finite element method. Compos. Struct. **46**(3), 197–208 (1999)
9. Chen, J., Dawe, D.J., Wang, S.: Nonlinear transient analysis of rectangular composite laminated plates. Compos. Struct. **49**(2), 129–139 (2000)
10. Lee, Y.Y., Ng, C.F.: Nonlinear response of composite plates using the finite element modal reduction method. Eng. Struct. **23**(9), 1104–1114 (2001)
11. Harras, B., Benamar, R., White, R.G.: Geometrically non-linear free vibration of fully clamped symmetrically laminated rectangular composite plates. J. Sound Vib. **251**(4), 579–619 (2002)
12. Onkar, A.K., Yadav, D.: Forced nonlinear vibration of laminated composite plates with random material properties. Compos. Struct. **70**(3), 334–342 (2005)
13. Singha, M.K., Daripa, R.: Nonlinear vibration of symmetrically laminated composite skew plates by finite element method. Int. J. Non Linear Mech. **42**(9), 1144–1152 (2007)
14. Kazancı, Zafer, Mecitoğlu, Zahit: Nonlinear dynamic behavior of simply supported laminated composite plates subjected to blast load. J. Sound Vib. **317**(3–5), 883–897 (2008)
15. Singha, M.K., Daripa, R.: Nonlinear vibration and dynamic stability analysis of composite plates. J. Sound Vib. **328**(4), 541–554 (2009)
16. Hahn, H.T., Tsai, S.W.: Nonlinear elastic behavior of unidirectional composite laminae. J. Compos. Mater. **7**(1), 102–118 (1973)
17. Jones, R.M., Nelson, D.A.R.: A new material model for the nonlinear biaxial behavior of atj-s graphite. J. Compos. Mater. **9**(1), 10–27 (1975)
18. Jones, R.M., Morgan, H.S.: Analysis of non-linear stress–strain behavior of fiber-reinforced composite materials. AIAA **15**, 1669–1676 (1977)
19. Amijima, S., Adachi, T.: Nonlinear stress-strain response of laminated composites. J. Compos. Mater. **13**(3), 206–218 (1979)
20. Mathison, S.R., Pindera, M.J., Herakovich, C.T.: Nonlinear response of resin matrix laminates using endochronic theory. J. Eng. Mater. Technol. **113**(4), 449–455 (1991)
21. Tabiei, A., Yi, W., Goldberg, R.: Non-linear strain rate dependent micro-mechanical composite material model for finite element impact and Crashworthiness simulation. Int. J. Non Linear Mech. **40**(7), 957–970 (2005)
22. Firle, T.E.: Amplitude dependence of internal friction and Shear modulus of Boron fibers. J. Appl. Phys. **39**(6), 2839–2845 (1968)
23. Maslov, K., Kinra, V.K.: Amplitude–frequency dependence of damping properties of carbon foams. J. Sound Vib. **282**(3), 769–780 (2005)
24. Höfer, P., Lion, A.: Modelling of frequency- and amplitude-dependent material properties of filler-reinforced rubber. J. Mech. Phys. Solids **57**(3), 500–520 (2009)
25. Khan, S.U., Li, C.Y., Siddiqui, N.A., et al.: Vibration damping characteristics of carbon fiber-reinforced composites containing multi-walled carbon nanotubes. Compos. Sci. Technol. **71**(12), 1486–1494 (2011)
26. Li, H., Niu, Y., Mu, C., et al.: Identification of loss factor of fiber-reinforced composite based on complex modulus method. Shock Vib. **2017**(2), 1–13 (2017)

Journal: **11071** MS: **4486** ☐ TYPESET ☐ DISK ☐ LE ☐ CP Disp.:**2018/7/31** Pages: **23** Layout: **Medium**

27. Arqub, O.A., Abo-Hammour, Z.: Numerical solution of systems of second-order boundary value problems using continuous genetic algorithm. Inf. Sci. **279**, 396–415 (2014)
28. Arqub, O.A.: The reproducing kernel algorithm for handling differential algebraic systems of ordinary differential equations. Math. Methods Appl. Sci. **39**(15), 4549–4562 (2016)
29. Kim, S.Y., Lee, D.H.: Identification of fractional-derivative-model parameters of viscoelastic materials from measured FRFs. J. Sound Vib. **324**(3), 570–586 (2009)
30. Johnson, C.D.: Characterization of damping properties of nonlinear viscoelastic materials. Proc. SPIE Int. Soc. Opt. Eng. **2445**, 200–211 (1995)

Journal: **11071** MS: **4486** TYPESET DISK LE CP Disp.:**2018/7/31** Pages: **23** Layout: **Medium**